Cerebral Cortex April 2005;15:361-370
doi:10.1093/cercor/bhh138
Advance Access publication July 21, 2004

Selective Postsynaptic Co-localization of MCT2 with AMPA Receptor GluR2/3 Subunits at Excitatory Synapses Exhibiting AMPA Receptor Trafficking

Linda Hildegard Bergersen[1,2], Pierre J. Magistretti[2] and Luc Pellerin[2]

[1]Anatomical Institute and the Centre for Molecular Biology and Neuroscience, University of Oslo, Blindern, Oslo, Norway and [2]Institut de Physiologie, 7 Rue du Bugnon, 1005 Lausanne, Switzerland

MCT2 is the main neuronal monocarboxylate transporter needed by neurons if they are to use lactate as an additional energy substrate. Previous evidence suggested that some MCT2 could be located in postsynaptic elements of glutamatergic synapses. Using post-embedding electron microscopic immunocytochemistry, it is demonstrated that MCT2 is present at postsynaptic density of asymmetric synapses, in the stratum radiatum of both rat hippocampal CA1 and CA3 regions, as well as at parallel fibre–Purkinje cell synapses in mouse cerebellum. MCT2 levels were significantly lower at mossy fibre synapses on CA3 neurons, and MCT2 was almost absent from symmetric synapses on CA1 pyramidal cells. It could also be demonstrated using quantitative double-labeling immunogold cytochemistry that MCT2 and AMPA receptor GluR2/3 subunits have a similar postsynaptic distribution at asymmetric synapses with high levels expressed within the postsynaptic density. In addition, as for AMPA receptors, a significant proportion of MCT2 is located on vesicular membranes within the postsynaptic spine, forming an intracellular pool available for a putative postsynaptic endo/exocytotic trafficking at these excitatory synapses. Altogether, the data presented provide evidence for MCT2 expression in the postsynaptic density area at specific subsets of glutamatergic synapses, and also suggest that MCT2, like AMPA receptors, could undergo membrane trafficking.

Keywords: energy metabolism, lactate, monocarboxylate transporter, postsynaptic density, synaptic plasticity

Introduction

Monocarboxylate transporters form a family of proton-linked transporters involved in the uptake and release of lactate, pyruvate and ketone bodies (for review, see Enerson and Drewes, 2003; Halestrap and Meredith, 2004). Of the 14 members described so far, three are clearly expressed in the central nervous system. MCT1 has been shown to be predominantly expressed by astrocytes, both *in vitro* (Hanu *et al.*, 2000; Debernardi *et al.*, 2003) and *in vivo* (Hanu *et al.*, 2000; Pierre *et al.*, 2000), as well as by endothelial cells forming blood vessels (Gerhart *et al.*, 1997) and by some restricted populations of neurons (Leino *et al.* 1999; Ainscow *et al.*, 2002; Debernardi *et al.*, 2003). MCT4 expression has been observed both on Bergmann glial cells in cerebellum (Bergersen *et al.*, 2001) as well as on hippocampal astrocytes (Rafiki *et al.*, 2003). In contrast, MCT2 was described as the predominant neuronal monocarboxylate transporter expressed on dendritic membranes forming the neuropil (Pierre *et al.*, 2002; Debernardi *et al.*, 2003). Based on a number of *in vitro* and *in vivo* studies, it has been proposed that these transporters could be involved in a process of lactate transfer between astrocytes and neurons (Pellerin, 2003). Moreover, it was postulated that MCT2 could play a particular role in enhancing neuronal lactate uptake at activated glutamatergic synapses. Consistent with this concept, MCT2 was found to be present in the postsynaptic density area (PSD) at parallel fibre–Purkinje cell synapses in the cerebellum (Bergersen *et al.*, 2001) and to be co-localized with PSD95, a PSD protein, in the cortex (Pierre *et al.*, 2002). Nevertheless, a more conclusive demonstration that MCT2, in addition to its general expression on dendritic membranes, could be located specifically in the PSD area of various types of glutamatergic synapses is still awaited.

Considering the critical role of AMPA receptors in synaptic transmission and plasticity, it is perhaps surprising that their synaptic distribution has only recently been a major focus of interest (for review, see Takumi *et al.*, 1998; Nusser, 2000). AMPA receptors are concentrated at glutamatergic synapses and they are never observed at postsynaptic membranes of GABAergic synapses. In addition, they are present at high density within the postsynaptic specialization with an abrupt reduction outside this zone. An important aspect of synaptic AMPA receptor distribution is the presence of an endogenous vesicular pool within postsynaptic spines and the demonstration that they undergo a process of translocation known as AMPA receptor trafficking (Malinow and Malenka, 2002; Bredt and Nicoll, 2003). Thus, AMPA receptors can be either inserted or removed from the postsynaptic membrane by specific mechanisms of exo- and endocytosis (Barry and Ziff, 2002). It has been postulated that these phenomena would subserve synaptic plasticity processes such as long-term potentiation (LTP) and long-term depression (LTD).

In this study, we determined the precise synaptic distribution of MCT2 at several asymmetric (excitatory) and symmetric (inhibitory) synapses using immunogold labeling and electron microscopy. Moreover, we compared both MCT2 and AMPA receptor GluR2/3 subunit distribution at different types of asymmetric synapses and made a parallel quantitative analysis of their expression as a function of the distance from the PSD area. Our data suggest a specific role of MCT2 at glutamatergic synapses and a link with AMPA receptor trafficking.

Materials and Methods

MCT2 and GluR2/3 Antibodies

MCT2 antibody production and characterization have been described previously (Pierre *et al.*, 2000, 2003). Briefly, one peptide consisting of the 15 carboxyl-terminal amino acids of rat MCT2 (CNTHNPPSDRDKESSI) was synthesized, with a cysteine added at the N-terminal site for optimal conjugation to Keyhole Limpet Hemocyanine. MCT2 antisera were obtained after subcutaneous injections of this peptide into two rabbits. Specificity of the MCT2 antibody was demonstrated in previous studies where it was used both for immunocytochemistry and Western

blot experiments. Peptide antigen has been used as a competitive inhibitor of anti-MCT2 antibody, by preabsorbing the MCT2 primary antibody with 10 μg/ml of the appropriate peptide antigen. Staining was absent on membranes or in sections that had been incubated in such a solution (Pierre *et al.*, 2000, 2002). In addition, specificity of the MCT2 antibody was further addressed by Western blot using fractions from different mouse tissues. The MCT2 antibody recognized a single band with molecular weight of 40–43 kDa in mouse brain, liver and kidney extracts, but not in striated muscle, heart, lung or stomach, in accordance with previous studies (Jackson *et al.*, 1997; Bergersen *et al.*, 2001).

The polyclonal GluR2/3 antibody initially developed by Wenthold (Wenthold *et al.*, 1992) was obtained commercially from Chemicon (AB1506). It has been generated using a peptide consisting of the 13 carboxy-terminal amino acids of the rat GluR2 (EGYNVYGIESVKI). Western blot analysis confirmed the labeling of a single band with a molecular weight of ~108 kDa as expected (data not shown).

Postembedding Immunogold Cytochemistry

Adult OF1 mice (20–50 g; $n = 3$) and adult male Wistar rats (250–300 g, $n = 4$ from Møllegaard, Ejby, Denmark) were used. All the animals were given free access to food and drinking water. All experiments were performed in accordance with guidelines of the Norwegian and Swiss Committees on Animal Experimentation. Animals were deeply anesthetized by an intraperitoneal injection of Equetisin (0.4 ml/100 g body wt) and subjected to transcardiac perfusion with 2% dextran (mol. wt 70 000) in 0.1 M sodium phosphate buffer (NaPi; pH 7.4, 4°C, 15 s), followed by a mixture of 0.1% glutaraldehyde and 4% formaldehyde (freshly depolymerized from paraformaldehyde) in 0.1 M NaPi (pH 7.4) at 4°C. The brain was left *in situ* overnight (4°C).

Small rectangular pieces (typically 0.5 × 0.5 × 1 mm) of brain tissue were cryoprotected by immersion in graded concentrations of glycerol (10, 20 and 30%) in 0.1 M NaPi for 30 min at each step and then overnight in 30% glycerol in 0.1 M NaPi at 4°C. Samples were then plunged into liquid propane cooled at –190°C with liquid nitrogen in a Universal Cryofixation System KF80 (Reichert-Jung, Wien, Austria). Tissue blocks were moved with precooled forceps. For freeze-substitution (Müller *et al.*, 1980), tissue samples were immersed in a solution of anhydrous methanol and 0.5% uranyl acetate overnight at –90°C. The temperature was raised stepwise in 4°C increments per hour from –90 to –45°C, where it was kept for the subsequent steps. Tissue samples were washed several times with anhydrous methanol to remove residual water and uranyl acetate. The infiltration in Lowicryl HM20 went stepwise from Lowicryl/methanol 1:2, 1:1 and 2:1 (1 h each) to pure Lowicryl (overnight). For polymerization, the tissue was placed in a precooled embedding mall. The polymerization was catalyzed by UV light at a wavelength of 360 nm for 2 days at –45°C followed by 1 day at room temperature. Ultrathin sections (70 nm) were cut with a diamond knife on a Reichert-Jung ultramicrotome and mounted on nickel grids using an adhesive pen (David Sangyo).

Grids with the ultrathin sections were processed at room temperature in solutions containing 50 mM Tris HCl buffer, pH 7.4, 0.05 M NaCl, and 0.1% Triton X-100 (TBST) and completed as stated below. Sections were first washed in TBST containing 0.1% sodium borohydride and 50 mM glycine for 10 min, followed by TBST containing 2% human serum albumin (HSA) for 10 min. They were then incubated overnight with primary antibodies diluted in TBST containing 2% HSA. The antibody against MCT2 (dilution: 1 μg/ml) as well as an antibody recognizing the glutamate receptor 2 and 3 subunits (GluR2/3) forming AMPA receptors (dilution: 2 μg/ml) were used. Goat anti-rabbit immunoglobulins coupled to 10 nm gold particles (Amersham, Arlington Heights, IL, USA) were diluted 1:20 in TBST with 2% HSA and 5 mg/ml polyethylene glycol. In double labeling experiments (Ottersen *et al.*, 1992), sections were treated with the antibody against MCT2 (dilution as above) in the first step (followed by a first gold-labeled secondary antibody) and with the AMPA receptor GluR2/3 subunit antibody (dilution as above) in the next one (revealed by another gold-labeled secondary antibody). Exposure to formaldehyde vapours (80° C, 1 h) was used between the two immunolabeling steps (Wang and Larsson, 1985). This treatment leads to the destruction by formaldehyde of the remaining free anti-IgG binding sites on the primary antibody against the first antigen. Potential cross-reactivity arising from the subsequent use of another secondary antibody that would be directed against the same species is prevented in this manner. Such a procedure allows the simultaneous detection of two different antigens when using two primary antibodies from the same species. MCT2 and AMPA receptor GluR2/3 subunits were distinguished by means of different gold particle sizes (10 nm for MCT2, 15 nm for GluR2/3 subunits). In some experiments, GluR2/3 subunits were revealed first and MCT2 after. The two double labeling approaches gave similar MCT2 and GluR2/3 subunit labeling patterns as the single labeling protocol.

Ultrathin sections were contrasted in uranyl acetate (20–40 min) and lead citrate (2–4 min), before they were observed in a Philips CM100 electron microscope. Pictures were usually taken at a primary magnification of 11 000×.

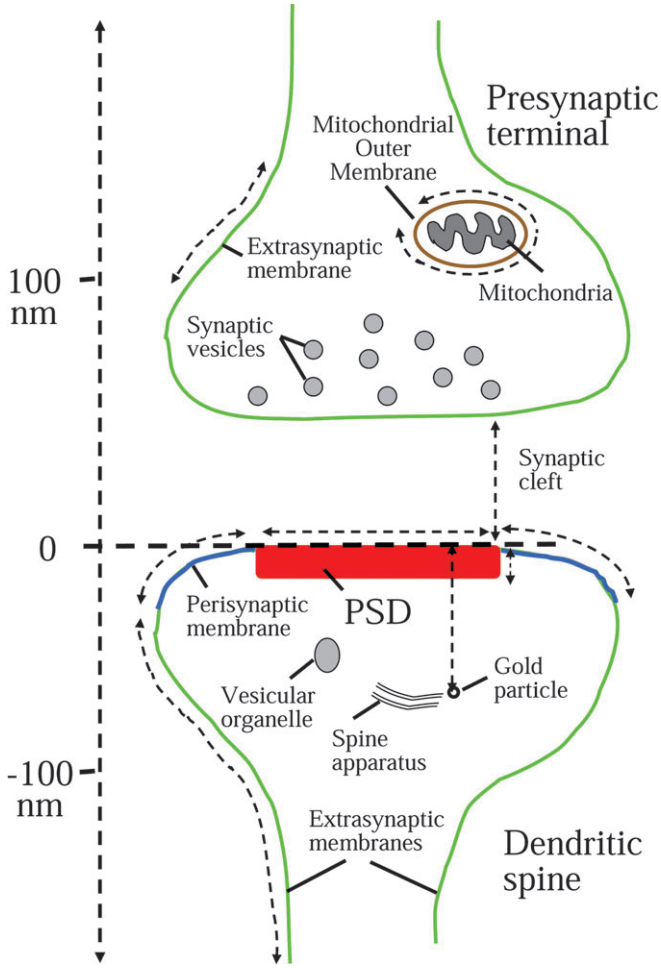

Figure 1. Schematic illustration of a synapse between a presynaptic terminal and a dendritic spine exhibiting an asymmetric specialization and some typical intracellular organelles as can be observed by electron microscopy. Analysis of gold particle density (number of gold particles/μm of membrane length) was performed in four specific membrane compartments that were defined as: the postsynaptic density (PSD; red), perisynaptic membranes on each side of the PSD (blue), extrasynaptic membranes corresponding to all pre- and postsynaptic membranes outside the PSD and perisynaptic membranes (green) and mitochondrial outer membranes (brown). Association of gold particles with both vesicular organelles and spine apparatus was also assessed. Distribution of gold particles as a function of the distance from the external face of the PSD along a perpendicular axis (in the left margin) was determined. Double-headed arrows represent the distances and membrane length that were measured including the width of the PSD and the synaptic cleft. Note that the length of perisynaptic membrane considered corresponds to half the total length of the PSD on each side.

Quantitative Analysis

Electron micrographs were randomly taken in the hippocampus, in the stratum radiatum of area CA1 and CA3 as well as in the stratum lucidum and in the dentate hilus. In the cerebellum, micrographs were taken in the molecular layer. Gold particles corresponding to MCT2 and AMPA receptor GluR2/3 subunits were quantified as number of gold particles/μm of membrane length in the following asymmetric synapses: in hippocampal Schaffer collateral synapses (CA1 area), recurrent collateral fibre synapses (CA3 area) and large mossy fibre synapses (stratum lucidum and the dentate hilus; for identification criteria of mossy fibre synapses, see Bergersen *et al.*, 2003) as well as in parallel fibre–Purkinje cell synapses of the cerebellum (for identification criteria of parallel fibre synapses, see Bergersen *et al.*, 2001). Specific membrane compartments have been defined and used for quantifications (see schematic illustration on Fig. 1 for a more comprehensive presentation). They correspond to the postsynaptic density (PSD), perisynaptic membranes (corresponding to membrane on each side of the PSD), extrasynaptic membranes (belonging to either presynaptic terminals or dendrites but excluding the PSD and perisynaptic membranes) and mitochondrial outer membranes (found in presynaptic terminals). Perisynaptic membranes were defined for convenience of measurement as half the width of the PSD for all synapses. It should be noted, however, that this approach does not rely upon any physiological evidence that it is indeed correctly representing the exact dimension of such a compartment at every type of synapse. Only synaptic profiles with clearly visible postsynaptic membrane and postsynaptic density were selected for quantitative analysis. In addition, only synapses which showed a density of MCT2 gold particles that was at least 5-fold higher than in mitochondrial outer membranes (background level) were included in the analysis.

The distance between the center of gold particles associated with MCT2 or GluR2/3 subunits and the external face of the postsynaptic density was determined along a perpendicular axis. All gold particles located within the postsynaptic dendritic spine and the presynaptic terminal were recorded. The width of both the postsynaptic density and the synaptic cleft was measured.

Results

MCT2 is Expressed on Dendritic Spines at Various Glutamatergic Synapses

Using the postembedding immunogold technique, the synaptic distribution of MCT2 was studied in parallel with GluR2/3 subunits at different types of synapses in the hippocampus as well as in the cerebellum. First, immunogold labeling of hippocampal sections showed that MCT2 is present, together with GluR2/3 subunits, at synapses with an asymmetric synaptic specialization characteristic of glutamatergic synapses in the stratum radiatum of area CA1 [Schaffer collateral/commissural synapses (SCC)] as well as in area CA3 [recurrent collateral/commissural synapses (RCC)] (Figs 2*A–D* and 3*A–D*). Similarly, a high density of MCT2 together with high levels of GluR2/3 subunits was observed at asymmetric synapses between parallel fibres (PF) and Purkinje cells in the cerebellum (Fig. 4*A–E*). At each of these types of glutamatergic synapses, expression of

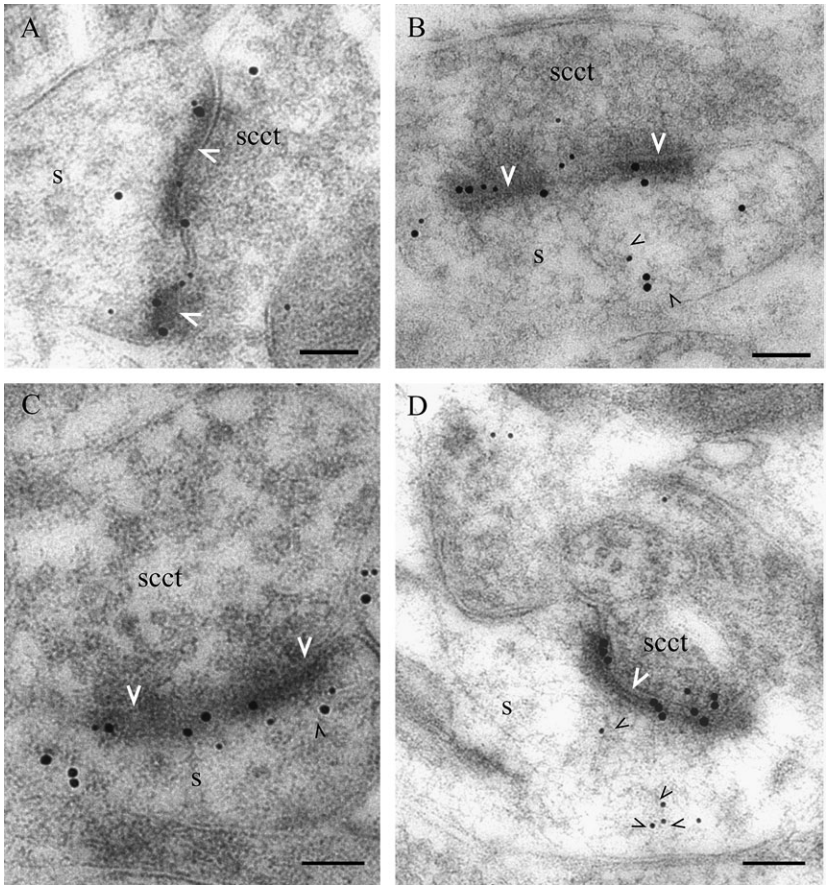

Figure 2. Localization of MCT2 and GluR2/3 subunits at Schaffer collateral/commissural fibre synapses in rat CA1 stratum radiatum by immunogold labeling. (*A–D*) Electron micrographs showing double labeling for MCT2 (small gold particles) and GluR2/3 subunits (large gold particles). Note the specific localization of MCT2 and GluR2/3 subunits in a restricted portion of the synaptic membrane at synapses (open white arrowheads) between Schaffer collateral/commissural fibre terminals (scct) and dendritic spines (s) corresponding to the postsynaptic density area, as well as in vesicular organelles (open arrowheads) within spines. Scale bars: 100 nm.

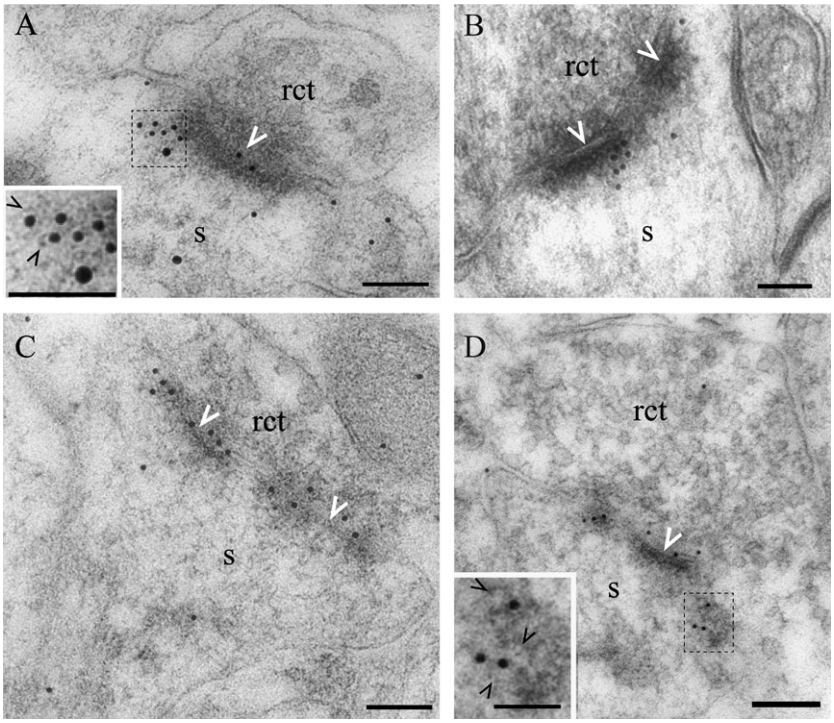

Figure 3. Localization of MCT2 and GluR2/3 subunits at recurrent collateral/commissural fibre synapses in the rat CA3 stratum radiatum by immunogold labeling. (*A*) Electron micrograph of a section double labeled for MCT2 (small gold particles) and GluR2/3 subunits (large gold particles). (*B*, *D*) Electron micrographs of single labeled sections for MCT2. Note that MCT2 and GluR2/3 subunits are detected not only in the postsynaptic density area at synapses (open white arrowheads) between recurrent collateral/commissural fibre terminals (rct) and dendritic spines (s), but also associated with vesicular membranes (open arrowheads) within spines. (*C*) Electron micrograph of a single labeled section for GluR2/3 subunits. Insets represent higher magnifications of areas indicated by dotted lines showing MCT2 (*A*, *D*) and GluR2/3 subunits (*A*) associated with vesicular membranes (arrowheads). Scale bars: *A*–C, 100 nm; *D*, 91 nm; inset *A*, 105 nm; inset *D*, 60 nm.

both MCT2 and GluR2/3 subunits appeared to be concentrated at the postsynaptic density area as other segments of plasma membrane (either in the presynaptic terminal or the postsynaptic spine) showed very low levels of gold particles.

In contrast to SCC, RCC and PF synapses, most mossy fibre synapses were immunonegative for MCT2, but displayed strong GluR2/3 subunits labeling as previously described (Fig. 5*A*; see also Nusser *et al.*, 1998; Takumi *et al.*, 1999). Nevertheless, some mossy fibre synapses exhibited a significant amount of MCT2 immunoreactivity, but levels were lower than those observed at the SCC, RCC and PF synapses (Fig. 5*B*). There was no difference in MCT2 content between mossy fibre synapses situated in the hilus of the dentate gyrus and those in the stratum lucidum of area CA3 (not shown). When the distribution of both MCT2 and GluR2/3 subunits was examined at symmetric synapses characteristic of GABAergic synapses within area CA1 of the hippocampus, expression of either MCT2 or GluR2/3 subunits detected in the postsynaptic membrane or elsewhere did not differ significantly from background levels (Fig. 5*C*,*D*). A quantitative assessment of the level of expression of MCT2 within postsynaptic density areas of all these different types of synapses confirmed the initial descriptive evaluation. While levels of MCT2 expression within postsynaptic areas were comparable between SCC, RCC and PF synapses, it was significantly reduced in mossy fibre synapses containing MCT2 (Fig. 6). Moreover, when the level of expression of MCT2 within each of these PSD areas was compared to other membrane segments as defined in Figure 1, it became clear that it was mostly confined to the PSD area (Fig. 6).

MCT2, Like AMPA Receptors, Is Not Only Enriched at the Postsynaptic Density but Is also Found within Dendritic Spines

In addition to its presence in the PSD area, it was noticed that MCT2, like AMPA receptors, also occurred within postsynaptic spines, which are often associated with vesicular organelles or the spine apparatus. Such a characteristic pattern of expression within dendritic spines has been associated previously to exo/endocytosis processes responsible for the insertion or removal of AMPA receptors from the postsynaptic membrane (Malinow and Malenka, 2002). Appearance of MCT2 together with AMPA receptor GluR2/3 subunits within spines was observed at synapses between SCC and CA1 pyramidal cells (Fig. 2*A*–*D*), between RCC and CA3 pyramidal cells (Fig. 3*A*–*D*) as well as between PF and Purkinje cells (Fig. 4*A*–*E*). This was particularly evident in large spines, which often harbored perforated synapses (Figs 2B, 3*B*,*C*). In some of these spines, MCT2 and GluR2/3 subunits could be seen in close association with the spine apparatus (Fig. 4*D*). In contrast, it was not the case at synapses between mossy fibres and CA3 pyramidal cells (Fig. 5*A*,*B*).

A precise quantitative distribution of both MCT2 and GluR2/3 subunits as a function of the distance from the PSD area, either in the direction of the presynaptic terminal or the postsynaptic spine, was undertaken at SCC, RCC and PF synapses (see Fig. 1 for a schematic illustration of what the measurements represent). As can be observed on each panel of Figure 7, the distribution of gold particles associated with either MCT2 or GluR2/3 subunits is significantly skewed in the postsynaptic

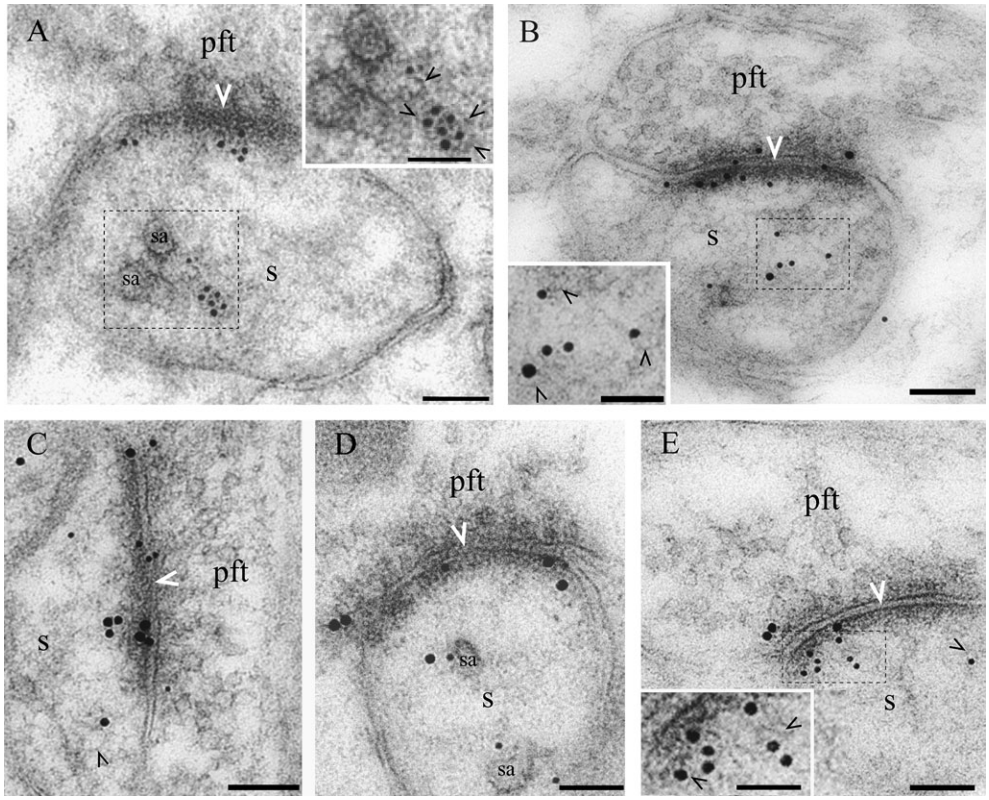

Figure 4. Localization of MCT2 and GluR2/3 subunits at parallel fibre–Purkinje cell synapses in the mouse cerebellar cortex by immunogold labeling. (*A*) Electron micrograph of a single labeled section for MCT2. (*B–E*) Electron micrographs of double labeled sections for MCT2 (small gold particles) and GluR2/3 subunits (large gold particles). Note that MCT2, like AMPA receptors, is present in the postsynaptic density area at synapses (open white arrowheads) between parallel fibre terminals (pft) and Purkinje cell dendritic spines (s), as well as on vesicular membranes (open arrowheads) within the postsynaptic spine. Within some spines, MCT2 labeling of membranous structures resembling the spine apparatus (sa) is visible. Insets, higher magnification of areas indicated by dotted lines showing MCT2 (*A*, *B*, *E*) and GluR2/3 subunit (*B*) positive vesicular membranes (arrowheads). Scale bars: 100 nm in *A* and *D*, 150 nm in *B*, *C* and *E*; insets, 75 nm in *A* and *B*, 50 nm in *E*.

direction. Gold particles were assigned to the PSD if they were located within 40 nm (which is similar to the lateral resolution of the immunogold method: see Chaudhry *et al.*, 1995; Nagelhus *et al.*, 1998) of the PSD borders (–40 to +40 on the *x*-axis). The mean postsynaptic distance between MCT2 or GluR2/3 subunit-associated gold particles and the extracellular face of the postsynaptic density is 63 nm and 51 nm at SCC synapses, 48 nm and 43 nm at RCC synapses, and 63 nm and 48 nm at PF synapses respectively. When the analysis of MCT2 and AMPA receptor GluR2/3 subunit distribution was restricted to gold particles that were confined within the PSD, MCT2 gold particles were located at a mean distance of 13 nm (SCC), 15 nm (RCC) and 17 nm (PF) from the extracellular face of the postsynaptic density, whereas the GluR2/3 subunits were located at a mean distance of 11, 12 and 13 nm respectively.

At the SCC and RCC synapses, the frequency analysis of the distribution of MCT2 immunogold particles perpendicular to the extracellular face of the postsynaptic density shows that the majority of gold particles (63.3 and 65.6% respectively) were located within 40 nm of the PSD border, and thus most likely belong to the postsynaptic density (Fig. 7 upper and middle panels, left). These proportions are similar to the values obtained for GluR2/3 subunits (78.3 and 78.9% respectively) (Fig. 7 upper and middle panels, right). Likewise, in the cerebellar PF synapses, 61.5 and 60.8% of gold particles associated with MCT2 and GluR2/3 subunits respectively belong to the PSD (Fig. 7 lower panel, left and right). Beyond 40 nm from the PSD area in the direction of the presynaptic terminal, very few, if any, gold particles associated with either MCT2 or GluR2/3 subunits were found. In contrast, in the opposite direction, i.e. from –40 nm to >–200 nm, a substantial proportion of gold particles associated with MCT2 (30, 26 and 29%) and GluR2/3 subunits (17, 16 and 28%) were located within dendritic spines at SCC, RCC and PF synapses respectively (Fig. 7). These data demonstrate that MCT2, like AMPA receptors, has a specific postsynaptic localization at the described synapses and they strongly suggest that a significant proportion is on its way to or getting away from the postsynaptic density area.

Discussion

MCT2 is a Novel PSD Protein at Glutamatergic Synapses

The postsynaptic density or PSD is a highly organized protein complex containing the biochemical machinery essential for carrying synaptic signals across the postsynaptic membrane (Gundelfinger and tom Dieck, 2000; Kennedy, 2000). It appears to contain several hundreds of proteins that belong to distinct categories (Yamauchi, 2002; Yoshimura *et al.*, 2004). They are grouped as receptors, ion channels, protein kinases and phosphatases, regulatory proteins, G proteins and related molecules, scaffold proteins, adaptor proteins, cytoskeletal elements, adhesion molecules or enzymes, as well as proteins belonging to other classes. Among the most important constituents of the

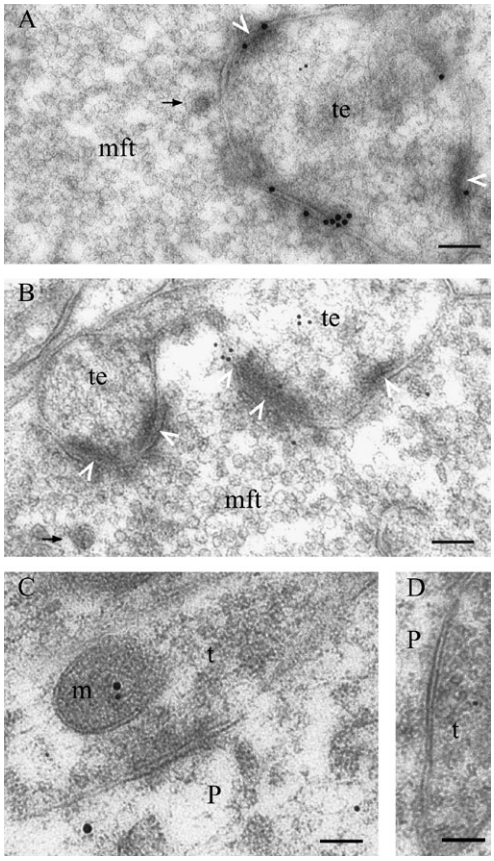

Figure 5. Double immunogold labelings for MCT2 (small gold particles) and GluR2/3 subunits (large gold particles) at asymmetric synapses between a mossy fibre terminal (mft) and a dendritic thorny excrescence (te) of a rat CA3 pyramidal cell (*A*, *B*), as well as at symmetric synapses between a terminal (t) and a rat CA1 pyramidal (P) cell body (*C*, *D*). Note the lack of MCT2 (small gold particle) labeling associated with the postsynaptic density area or within the dendritic spine in either asymmetric, GluR2/3 subunit positive synapses (open white arrowheads) (*A*, *B*) or symmetric, GluR2/3 subunit negative synapses (*C*, *D*). Arrows: neuropeptide containing dense core vesicles typically found in mossy fibre terminals; m: mitochondria. Scale bars: 150 nm in *A* and 75 nm in *B*, *C* and *D*.

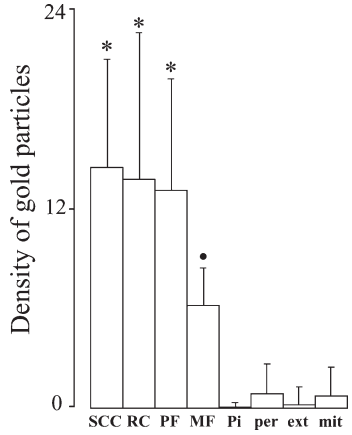

Figure 6. Quantitative assessment of MCT2 distribution between postsynaptic density areas of various excitatory and inhibitory synapses, as well as among different postsynaptic or mitochondrial membrane portions. Values along the abscissa give the density of gold particles associated with MCT2 (mean number of gold particles/μm of membrane portion ± SD). SCC, Schaffer collateral/commissural fibre synapses in rat CA1 ($n = 42$). RC, recurrent collateral/commissural fibre synapses in rat CA3 ($n = 30$). PF, mouse cerebellar parallel fibre/Purkinje cell synapses ($n = 31$). MF, mossy fibre synapses ($n = 23$). Pi, synapses with symmetric synaptic specializations on rat CA1 pyramidal cell bodies ($n = 15$). per, perisynaptic membranes of asymmetric synapses in rat hippocampus and mouse cerebellum, i.e. membrane adjacent to the postsynaptic density area equivalent to the latter in length ($n = 103$). ext, extrasynaptic membranes of dendrites postsynaptic to the excitatory synapses and of presynaptic terminals ($n = 103$). mit, outer membranes of mitochondria in presynaptic terminals (n = 85). Asterisks, values of SCC, RC and PF were significantly higher than those of MF ($P < 0.01$; non-parametric Mann–Whitney *U*-test). Filled circle, values of MF were significantly higher than those of per, ext and mit ($P < 0.01$; non-parametric Mann–Whitney *U*-test).

PSD are the different AMPA and NMDA receptor subunits; this should come as no surprise considering the crucial role these subunits play in synaptic transmission at glutamatergic synapses (Takumi *et al.*, 1999; Nusser 2000). In contrast, our finding that MCT2, a proton-linked monocarboxylate transporter involved in energy metabolism, is expressed at the PSD represents a quite unexpected observation. Indeed, transporters in general or proteins involved in energy metabolism have rarely been reported to be associated with the PSD. In a previous study, Bergersen *et al.* (2001) observed the presence of MCT2 at the PSD of parallel fibre–Purkinje cell synapses in rat cerebellum. Moreover, although they failed to find extensive co-localization with some synaptic proteins, Pierre *et al.* (2002) reported in mouse cerebral cortex a certain degree of co-localization between MCT2 and PSD95, a major constituent of PSD at glutamatergic synapses, thus suggesting a wider association of MCT2 with the PSD of various types of synapses. Data presented here clarify this issue and further extend these previous observations, undoubtedly demonstrating that some MCT2 is located at the PSD of distinct glutamatergic synapses, but is not present at GABAergic synapses. Such a distribution was found to be similar to the synaptic distribution of the GluR2/3 subunits, which are components of AMPA receptors, and are expressed at the PSD of various glutamatergic but not GABAergic synapses (Takumi *et al.*, 1999; Nusser 2000). One intriguing observation, however, is the fact that at mossy fibre synapses, which are known to express high levels of AMPA receptors but low levels of NMDA receptors, MCT2 is often absent, or when present its levels of expression are significantly lower than at other glutamatergic synapses. Although no specific explanation can as yet be provided, it is interesting to note that the hippocampal

Figure 7. Frequency plots for the spatial distribution of MCT2 and GluR2/3 subunits as a function of the distance from the postsynaptic density area at excitatory synapses. The frequency histograms show the distribution, as a function of the distance from the external face of the postsynaptic density, of MCT2 and GluR2/3 subunit-associated gold particles at asymmetric synapses between nerve terminals and dendritic spines in stratum radiatum of CA1 (SCC) and CA3 (RC) areas as well as in the cerebellar molecular layer (PF). The distance from the center of gold particles to the external face of the postsynaptic density was recorded perpendicularly to the postsynaptic membrane (see illustration in Fig. 1). All gold particles located within the postsynaptic spine and the presynaptic terminal (excluding those belonging to extrasynaptic plasma membranes) were included in the analysis. Numbers of gold particles that were considered in the analysis are as follows: for SCC, $n = 244$ gold particles for MCT2 and $n = 208$ gold particles for GluR2/3 subunits; for RC, $n = 128$ gold particles for both MCT2 and GluR2/3 subunits; for PF, $n = 270$ gold particles for MCT2 and $n = 199$ gold particles for GluR2/3 subunits. The average width of the postsynaptic density (psd; 29 nm) and synaptic cleft (sc; 16 nm) is indicated under each plot. Because the lateral resolution of the immunogold method is ~40 nm (Chaudhry *et al.*, 1995; Nagelhus *et al.*, 1998), gold particles located within this distance on either the presynaptic side of the extracellular postsynaptic density border or on the postsynaptic side of the intracellular postsynaptic density border were considered to signal epitopes in the postsynaptic density itself.

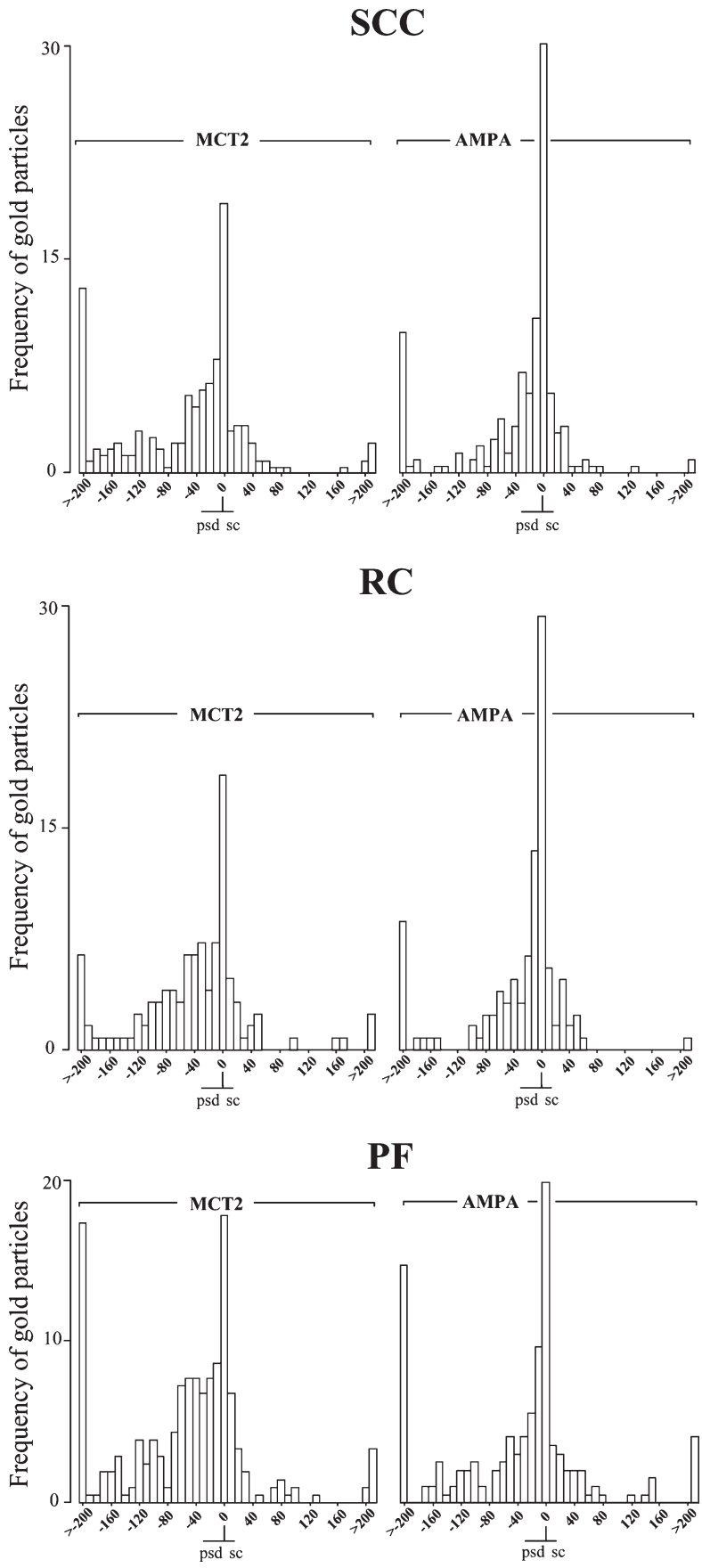
SCC
RC
PF
MCT2
AMPA
Frequency of gold particles
psd sc
>-200
-160
-120
-80
-40
0
40
80
120
160
>200

mossy fibre pathway exhibits distinct features compared to Schaffer collateral or recurrent/commissural pathways. Granule cells from which mossy fibres arise do not sustain prolonged high-frequency bursts under normal physiological conditions; moreover, mossy fibre synapses undergo forms of long-term plasticity that are NMDA receptor-independent and have a presynaptic site of expression (Henze *et al.*, 2000; Urban *et al.*, 2001). Whether such characteristics could determine specific aspects related to energy metabolism is a consideration that remains to be further explored.

Trafficking of a Monocarboxylate Transporter with AMPA Receptors at the Postsynaptic Membrane

In addition to their expression at the PSD of glutamatergic synapses, AMPA receptors have been found to be present in an intracellular membrane compartment composed of round and tubular vesicles (Lee *et al.*, 2001). Furthermore, both light and electron microscopic studies have revealed the presence of AMPA receptor pools within dendritic spines (Kessler and Baude, 1999; Shi *et al.*, 1999; Greger *et al.*, 2002). Results reported here are consistent with these observations in three distinct glutamatergic synapses, the Schaffer collateral–CA1 pyramidal neuron and the recurrent/commissural–CA3 pyramidal neuron synapses in the hippocampus as well as the parallel fibre–Purkinje cell synapse in the cerebellum. Interestingly, the monocarboxylate transporter MCT2 also exhibited expression on vesicular structures within dendritic spines of the same glutamatergic synapses in parallel with AMPA receptor GluR2/3 subunits. This remarkable similarity in distribution suggests that MCT2 might participate in the same translocation processes that AMPA receptors undergo at these synapses.

A major breakthrough in our understanding of the mechanisms at play in different forms of synaptic plasticity such as long-term potentiation and long-term depression came when it was shown that AMPA receptors undergo what is known as AMPA receptor trafficking (Barry and Ziff, 2002; Bredt and Nicoll, 2003). Specific processes for both insertion and removal of AMPA receptors into and out of the postsynaptic membrane have been described, together with a series of proteins including some directly interacting with AMPA receptor subunits such as ABP/GRIP, Pick1, SAP97, NSF or Stargazin (Henley, 2003). MCT2 seems to constitute a novel companion for AMPA receptor trafficking although no evidence exists at the moment for a direct interaction with one of these proteins or with AMPA receptor subunits themselves. Moreover, we cannot exclude for the moment that MCT2 and GluR2/3 subunits could translocate to the postsynaptic membrane via distinct mechanisms. Interestingly, a specific distinction has been made between GluR1/2 and GluR2/3 heteromers constituting AMPA receptors in their ability to translocate to the postsynaptic membrane. Thus, it was shown that GluR1/2 heteromer insertion into the postsynaptic membrane is driven by stimuli capable of inducing plasticity and can occur at extrasynaptic sites (Shi *et al.*, 1999; Hayashi *et al.*, 2000). In contrast, GluR2/3 heteromers are inserted in a constitutive manner exclusively in the PSD, replacing previously inserted heteromers (Passafaro *et al.*, 2001; Shi *et al.*, 2001). From the present distribution data showing a parallel between MCT2 and GluR2/3 subunits, it could be argued that MCT2 might share a similar fate as GluR2/3 heteromers, i.e. participating in a constitutive mechanism of exo/endocytosis. It cannot be excluded, however, that MCT2 expression at the PSD could be also enhanced/decreased upon induction of plasticity, as occurs for GluR1/2 heteromers.

Another observation supports the view that MCT2 might participate in AMPA receptor trafficking. In a previous study, it was shown that MCT2 co-localizes at parallel fibre–Purkinje cell synapses with the δ2-glutamate receptors (Bergersen *et al.*, 2001). Very little is known about the specific role of this orphan glutamate receptor, which does not bind glutamate analogs and does not form functional glutamate-gated ion channels (Yamazaki *et al.*, 1992; Lomeli *et al.*, 1993; Mayat *et al.*, 1995). In a recent report, Hirai *et al.* (2003) showed that δ2-glutamate receptors prevent AMPA receptor endocytosis at PF synapses, and as a consequence are essential for maintaining synaptic transmission while being involved in long-term depression, a major form of plasticity at these synapses. Thus, MCT2 could also participate, together with the δ2-glutamate receptor, in AMPA receptor trafficking at PF synapses, either as a simple co-passenger with AMPA receptors or as a critical component of the mechanism subserving synaptic plasticity. It remains to be demonstrated, however, whether MCT2 could interact directly with the δ2-glutamate receptor.

Functional Significance

The data presented here demonstrate that a fraction of MCT2 proteins are located at dendritic spines of specific glutamatergic synapses. Considering the function of MCT2 as a monocarboxylate carrier, it is tempting to suggest that its major role could be to maintain energy substrate availability upon excitation of postsynaptic cells by glutamate via AMPA receptor activation. Lactate, the major monocarboxylate found in the adult brain, has been shown recently to be a preferential oxidative substrate for neurons (Bouzier-Sore *et al.*, 2003; Itoh *et al.*, 2003). Moreover, a purported mechanism to ensure sufficient energy supply to neurons has been described whereby astrocytes respond to glutamatergic activity by releasing more lactate in the extracellular space (Pellerin and Magistretti, 1994). Evidence that Bergmann glial cells in the cerebellum have processes expressing MCT4, another monocarboxylate transporter expressed by lactate producing cells, in close proximity to PF synapses expressing MCT2, further supports this view (Bergersen *et al.*, 2001). Combined with recent evidence demonstrating neurotransmitter-induced enhancement in MCT2 protein expression in neurons (Pierre *et al.*, 2003), our data suggesting that MCT2 could be inserted into the postsynaptic membrane together with AMPA receptors would provide an elegant mechanism to further tie activity and energy demands with supply at glutamatergic synapses.

Notes

L.H.B. was the recipient of a postdoctoral fellowship from the Norwegian Medical Research Council. This work was supported by grant no. 3100A0-100679 from Swiss Fonds National de la Recherche Scientifique to L.P.

Address correspondence to Dr Luc Pellerin, Institut de Physiologie, 7 rue du Bugnon, 1005 Lausanne, Switzerland. Email: luc.pellerin@iphysiol.unil.ch.

References

Ainscow EK, Mirshamsi S, Tang T, Ashford ML, Rutter GA (2002) Dynamic imaging of free cytosolic ATP concentration during fuel sensing by rat hypothalamic neurones: evidence for ATP-independent control of ATP-sensitive K(+) channels. J Physiol 544:429–445.

Barry MF, Ziff EB (2002) Receptor trafficking and the plasticity of excitatory synapses. Curr Opin Neurobiol 12:279–286.
Bergersen L, Wærhaug O, Helm J, Thomas M, Laake P, Davies AJ, Wilson MC, Halestrap AP, Ottersen OP (2001) A novel postsynaptic density protein: the monocarboxylate transporter MCT2 is co-localized with delta-glutamate receptors in postsynaptic densities of parallel fibre-Purkinje cell synapses. Exp Brain Res 136:523–534.
Bergersen L, Rafiki A, Ottersen OP (2002) Immunogold cytochemistry identifies specialized membrane domains for monocarboxylate transport in the central nervous system. Neurochem Res 27:89–96.
Bergersen L, Ruiz A, Bjaalie JG, Kullmann DM, Gundersen V (2003) GABA and GABAa receptors at hippocampal mossy fibre synapses. Eur J Neurosci 18:931–941.
Bouzier-Sore AK, Voisin P, Canioni P, Magistretti PJ, Pellerin L (2003) Lactate is a preferential oxidative energy substrate over glucose for neurons in culture. J Cereb Blood Flow Metab 23:1298–1306.
Bredt DS, Nicoll RA (2003) AMPA receptor trafficking at excitatory synapses. Neuron 40:361–379.
Chaudhry FA, Lehre KP, Van Lookeren Campagne M, Ottersen OP, Danbolt NC, Storm-Mathisen J (1995) Glutamate transporters in glial plasma membranes: highly differentiated localizations revealed by quantitative ultrastructural immunocytochemistry. Neuron 14: 711–720.
Debernardi R, Pierre K, Lengacher S, Magistretti PJ, Pellerin L (2003) Cell-specific expression pattern of monocarboxylate transporters in astrocytes and neurons observed in different mouse brain cortical cell cultures. J Neurosci Res 73:141–155.
Enerson BE, Drewes LR (2003) Molecular features, regulation, and function of monocarboxylate transporters: implications for drug delivery. J Pharm Sci 92:1531–1544.
Gerhart DZ, Enerson BE, Zhdankina OY, Leino RL, Drewes LR (1997) Expression of monocarboxylate transporter MCT1 by brain endothelium and glia in adult and suckling rats. Am J Physiol 273: E207–E213.
Greger IH, Khatri L, Ziff EB (2002) RNA editing at arg607 controls AMPA receptor exit from the endoplasmic reticulum. Neuron 34:759–772.
Gundelfinger ED, tom Dieck S (2000) Molecular organization of excitatory chemical synapses in the mammalian brain. Naturwissenschaften 87:513–523.
Halestrap AP, Meredith D (2004) The SLC16 gene family-from monocarboxylate transporters (MCTs) to aromatic amino acid transporters and beyond. Pflugers Arch (in press).
Hanu R, McKenna M, O'Neill A, Resneck WG, Bloch RJ (2000) Monocarboxylic acid transporters, MCT1 and MCT2, in cortical astrocytes *in vitro* and *in vivo*. Am J Physiol 278:C921–C930.
Hayashi Y, Shi SH, Esteban JA, Piccini A, Poncer JC, Malinow R (2000) Driving AMPA receptors into synapses by LTP and CaMKII: requirement for GluR1 and PDZ domain interaction. Science 287: 2262–2267.
Henley JM (2003) Proteins interactions implicated in AMPA receptor trafficking: a clear destination and an improving route map. Neurosci Res 45:243–254.
Henze DA, Urban NN, Barrionuevo G (2000) The multifarious hippocampal mossy fiber pathway: a review. Neuroscience 98:407–427.
Hirai H, Launey T, Mikawa S, Torashima T, Yanagihara D, Kasaura T, Miyamoto A, Yuzaki M (2003) New role of delta2-glutamate receptors in AMPA receptor trafficking and cerebellar function. Nat Neurosci 6:869–876.
Itoh Y, Esaki T, Shimoji K, Cook M, Law MJ, Kaufman E, Sokoloff L (2003) Dichloroacetate effects on glucose and lactate oxidation by neurons and astroglia *in vitro* and on glucose utilization by brain *in vivo*. Proc Natl Acad Sci U S A 100:4879–4884.
Jackson VN, Price NT, Carpenter L, Halestrap AP (1997) Cloning of the monocarboxylate transporter isoform MCT2 from rat testis provides evidence that expression in tissues is species-specific and may involve post-transcriptional regulation. Biochem J 324:447–453.
Kennedy MB (2000) Signal-processing machines at the postsynaptic density. Science 290:750–754.
Kessler JP, Baude A (1999) Distribution of AMPA receptor subunits GluR1-4 in the dorsal vagal complex of the rat: a light and electron microscope immunocytochemical study. Synapse 34:55–67.
Lee SH, Valtschanoff JG, Kharazia VN, Weinberg R, Sheng M (2001) Biochemical and morphological characterization of an intracellular membrane compartment containing AMPA receptors. Neuropharmacology 41:680–692.
Leino RL, Gerhart DZ, Drewes LR (1999) Monocarboxylate transporter (MCT1) abundance in brains of suckling and adult rats: a quantitative electron microscopic immunogold study. Brain Res Dev Brain Res 113:47–54.
Lomeli H, Sprengel R, Laurie DJ, Kohr G, Herb A, Seeburg PH, Wisden W (1993) The rat delta-1 and delta-2 subunits extend the excitatory amino acid receptor family. FEBS Lett 315:318–322.
Malinow R, Malenka RC (2002) AMPA receptor trafficking and synaptic plasticity. Annu Rev Neurosci 25:103–126.
Mayat E, Petralia RS, Wang YX, Wenthold RJ (1995) Immunoprecipitation, immunoblotting, and immunocytochemistry studies suggest that glutamate receptor delta subunits form novel postsynaptic receptor complexes. J Neurosci 15:2533–2546.
Müller M, Marti T, Kriz S (1980) Improved structural preservation by freeze- substitution. Proceedings of the 7th European Congress on Electron Microscopy 2:720–721.
Nagelhus EA, Veruki ML, Torp R, Haug FM, Laake JH, Nielsen S, Agre P, Ottersen OP (1998) Aquaporin-4 water channel protein in the rat retina and optic nerve: polarized expression in Muller cells and fibrous astrocytes. J Neurosci 18:2506–2519.
Nusser Z (2000) AMPA and NMDA receptors: similarities and differences in their synaptic distribution. Curr Opin Neurobiol 10:337–341.
Nusser Z, Lujan R, Laube G, Roberts JD, Molnar E, Somogyi P (1998) Cell type and pathway dependence of synaptic AMPA receptor number and variability in the hippocampus. Neuron 21:545–559.
Ottersen OP, Zhang N, Walberg F (1992) Metabolic compartmentation of glutamate and glutamine: morphological evidence obtained by quantitative immunocytochemistry in rat cerebellum. Neuroscience 46:519–534.
Passafaro M, Piech V, Sheng M (2001) Subunit-specific temporal and spatial patterns of AMPA receptor exocytosis in hippocampal neurons. Nat Neurosci 4:917–926.
Pellerin L (2003) Lactate as a pivotal element in neuron-glia metabolic cooperation. Neurochem Int 43:331–338.
Pellerin L, Magistretti PJ (1994) Glutamate uptake into astrocytes stimulates aerobic glycolysis: a mechanism coupling neuronal activity to glucose utilization. Proc Natl Acad Sci USA 91: 10625–10629.
Pierre K, Pellerin L, Debernardi R, Riederer BM, Magistretti PJ (2000) Cell-specific localization of monocarboxylate transporters, MCT1 and MCT2, in the adult mouse brain revealed by double immunohistochemical labelling and confocal microscopy. Neuroscience 100:617–627.
Pierre K, Magistretti PJ, Pellerin L (2002) MCT2 is a major neuronal monocarboxylate transporter in the adult mouse brain. J Cereb Blood Flow Metab 22:586–595.
Pierre K, Debernardi R, Magistretti PJ, Pellerin L (2003) Noradrenaline enhances monocarboxylate transporter 2 expression in cultured mouse cortical neurons via a translational regulation. J Neurochem 86:1468–1476.
Rafiki A, Boulland JL, Halestrap AP, Ottersen OP, Bergersen L (2003) Highly differential expression of MCT2 and MCT4 protein in astroglia and neurons in the developing rat brain. Neuroscience 122:677–688.
Shi SH, Hayashi Y, Petralia RS, Zaman SH, Wenthold RJ, Svoboda K, Malinow R (1999) Rapid spine delivery and redistribution of AMPA receptors after synaptic NMDA receptor activation. Science 284:1811–1816.
Shi S, Hayashi Y, Esteban JA, Malinow R (2001) Subunit-specific rules governing AMPA receptor trafficking to synapses in hippocampal pyramidal neurons. Cell 105:331–43.
Takumi Y, Bergersen L, Landsend AS, Rinvik E, Ottersen OP (1998) Synaptic arrangement of glutamate receptors. Prog Brain Res 116:105–121.
Takumi Y, Ramirez-Leon V, Laake P, Rinvik E, Ottersen OP (1999) Different modes of expression of AMPA and NMDA receptors in hippocampal synapses. Nat Neurosci 2:618–624.

Urban NN, Henze DA, Barrionuevo G (2001) Revisiting the role of the hippocampal mossy fiber synapse. Hippocampus 11:408–417.
Wang BL, Larsson LI (1985) Simultaneous demonstration of multiple antigens by indirect immunofluorescence or immunogold staining. Novel light and electron microscopical double and triple staining method employing primary antibodies from the same species. Histochemistry 83:47–56.
Wenthold RJ, Yokotani N, Doi K, Wada K (1992) Immunochemical characterization of the non-NMDA glutamate receptor using subunit-specific antibodies. Evidence for a hetero-oligomeric structure in rat brain. J Biol Chem 267:501–507.
Yamauchi T (2002) Molecular constituents and phosphorylation-dependent regulation of the post-synaptic density. Mass Spectrom Rev 21:266–286.
Yamazaki M, Araki K, Shibata A, Mishina M (1992) Molecular cloning of a cDNA encoding a novel member of the mouse glutamate receptor channel family. Biochem Biophys Res Commun 183:886–892.
Yoshimura Y, Yamauchi Y, Shinkawa T, Taoka M, Donai H, Takahashi N, Isobe T, Yamauchi T (2004) Molecular constituents of the post-synaptic density fraction revealed by proteomic analysis using multi-dimensional liquid chromatography-tandem mass spectrometry. J Neurochem 88:759–768.